npj | robotics

Article

https://doi.org/10.1038/s44182-026-00097-w

Inductively triggered capsule robot for needle-based drug delivery

Check for updates

Lukas Masjosthusmann & Sarthak Misra ✉

Existing capsule robots designed to deliver drugs typically release them into the gastrointestinal lumen, where transport into the tissue depends on passive diffusion across physiological barriers such as the epithelial layer. This limits delivery efficiency. Needle-based delivery can bypass these barriers but requires compact actuation mechanisms that generate multi-newton forces while supporting untethered operation and magnetic steering. Here we present a programmable millimeter-scale capsule robot for needle-based drug delivery enabled by thermally triggered magnetic springs (TTMS). Each TTMS consists of a preloaded magnetic spring and a temperature-responsive locking structure whose trigger temperature can be programmed during fabrication. This enables multi-step sequential actuation using a single global thermal stimulus. The milli-scale capsule robot, featuring multiple TTMS, performs controlled needle ejection, fluid injection, and needle retraction. Contactless triggering is achieved through inductive heating and magnetic steering using an external magnet. Experiments demonstrate programmable thermal response and sufficient force for penetration of soft tissue mimics and ex vivo. Controlled locomotion is demonstrated in complex three-dimensional ex vivo environments. Together, these results establish TTMS as a promising actuation strategy for multifunctional capsule robots and demonstrate a programmable capsule robot capable of inductively triggered needle-based drug delivery.

The invasiveness of conventional endoscopic procedures for diagnosing and treating gastrointestinal (GI) disorders causes patient discomfort, increases the risk of tissue injury, and requires general anesthesia[1]. These limitations have motivated the development of ingestible capsule robots that provide untethered access to the GI tract with substantially reduced invasiveness compared to conventional interventions[2–4].

Early capsule robots relied on passive transport driven by natural peristalsis to perform imaging and environmental sensing tasks with limited controllability[5–10]. The introduction of external magnetic actuation has since enabled contactless steering of diagnostic capsules[11–14]. Building on these advances, recent research has increasingly shifted toward therapeutic functionality, including targeted drug delivery[15,16], biopsy[17,18], and microbiota sampling[19–21].

Among therapeutic applications, targeted drug delivery is of particular interest because it can increase therapeutic efficacy while reducing systemic exposure and off-target accumulation[22]. Magnetically actuated capsule robots can deliver payloads to a target location within the gastrointestinal tract in a controlled manner[23–28]. Soft and hydrogel-based designs extend this capability by enabling robot-level shape adaptation to biological environments[29–31]. However, most approaches rely on passive diffusion of the loaded drug across physiological barriers such as the mucus or epithelial layer, whose natural function is to protect underlying tissue from toxins and bacteria[32]. This limits delivery efficiency and restricts the classes of drugs that can be administered orally[33].

Injection-based drug delivery can physically bypass physiological barriers and deliver therapeutics directly into underlying tissue[34]. However, integrating injection mechanisms in capsule robots requires actuation mechanism capable of generating sufficient and controllable forces within a millimeter-scale untethered system compatible with magnetic navigation. Experimental studies report tissue puncture forces typically on the order of 1 N, with median values around 1.2 N and values extending into the multi-newton range depending on needle geometry and tissue properties[35]. Passive actuation mechanisms utilizing preloaded mechanical springs triggered by environmental changes, such as pH variations in the surrounding medium, can generate sufficient forces to inject a loaded drug[36–38]. However, passively triggered mechanisms provide limited spatial control and carry the risk of premature actuation, restricting clinical applicability.

Magnetically triggered actuation mechanisms have been proposed to improve controllability, but existing approaches face fundamental trade-offs. Systems with integrated reed sensors can be triggered by weak magnetic

Surgical Robotics Laboratory, University of Twente, Enschede, The Netherlands.
✉e-mail: s.misra@utwente.nl

fields (e.g., 0.5 mT), which enables remote control but restricts magnetic steering[39]. Alternatively, magnetic fields can be used directly to generate forces within the capsule. However, the actuation forces required for tissue puncture necessitate significantly larger magnetic fields (e.g., ~200 mT)[40]. One approach to increase the achievable actuation force is the use of impact-based mechanisms generating pulsed rather than continuous puncture forces[41,42], though these have not been demonstrated for drug delivery. However, whether using continuous or pulsed actuation, the maximum puncture force is limited by the performance of external actuation systems, especially in clinical-scale workspaces[43]. Consequently, there remains a need for an actuation strategy that can locally generate multi-newton forces while preserving magnetic steering and controllable triggering.

In this work, we present a programmable millimeter-scale capsule robot for needle-based drug delivery, enabled by thermally triggered magnetic springs (TTMS) (Fig. 1a). A comparison with representative capsule robots equipped with needles is provided in Supplementary Table 1. TTMS are compact actuation mechanisms that combine preloaded magnetic springs with temperature-responsive locking structures (Fig. 1b). When a design-specific trigger temperature is reached, the locking structure releases the magnetic spring, converting stored potential energy into pushing or pulling forces independent of external magnetic fields. The trigger temperature can be programmed during fabrication by adjusting the curing conditions of the locking structure, allowing geometrically identical TTMS to activate at different temperatures. This enables the design of programmable actuation sequences that are triggered by a single global thermal stimulus. In our system, this thermal stimulus is provided through inductive heating, which causes the capsule robot to perform a controlled multi-step actuation sequence that ejects a needle, releases a liquid payload, and subsequently retracts the needle. Decoupled from actuation or triggering, the capsule robot can be magnetically steered through constrained three-dimensional environments. Together, these capabilities enable a programmable capsule robot that combines magnetic navigation with inductively controlled needle-based drug delivery within the gastrointestinal tract.

Results

Programmable thermally triggered magnetic springs

In this work, programmable thermally triggered magnetic springs (TTMS) are introduced as a local actuation mechanism capable of generating forces of multiple newtons in milli-sized capsule robots (Fig 1b). In the context of needle-based drug delivery, forces in the range of 1-3 N are required to puncture soft tissue with an 18G needle[44]. Achieving such force levels using external magnetic actuation is challenging, as the magnetic force rapidly decreases with increasing distance from the magnetic source ($\mathbf{F}_m \propto 1/L^4$), requiring either large magnets or, for external actuation impractical small source-to-capsule distances (Fig. 2a and Supplementary Note 1). TTMS overcome this limitation by generating force locally within the capsule, independent of externally applied magnetic forces.

TTMS consists of a preloaded magnetic spring formed by at least two permanent magnets, one of which is free to translate, and a thermally responsive locking structure fabricated from NOA63 (Norland Products, USA). NOA63 is a biocompatible shape memory polymer with stiffness that depends on both the cure temperature (T_c) and the ambient temperature (T_a)[45,46]. Higher curing temperatures permanently increase the stiffness of the material, while increasing the ambient temperature temporarily softens the material. NOA63-based millimeter-scale compliant structures have been shown to maintain their mechanical response under repeated actuation, with less than 2.5% reduction in resulting deformation observed after 50 actuation cycles[47]. As the locking structure softens upon heating, potential energy stored in the preloaded magnetic spring can be released on demand. Based on the orientation of the embedded magnetic spring, TTMS can generate either pushing or pulling forces.

The operating principle of TTMS is first demonstrated using a simplified locking structure (Fig. 2b and Supplementary Fig. 4). The simplified TTMS consists of two cylindrical NOA63 beams and two repelling ring magnets that generate a magnetic force of 0.8 N at a separation of 1 mm (Fig. 2c). The lower magnet shown in Fig. 2b is fixed in position, while the upper magnet is guided by a central non-

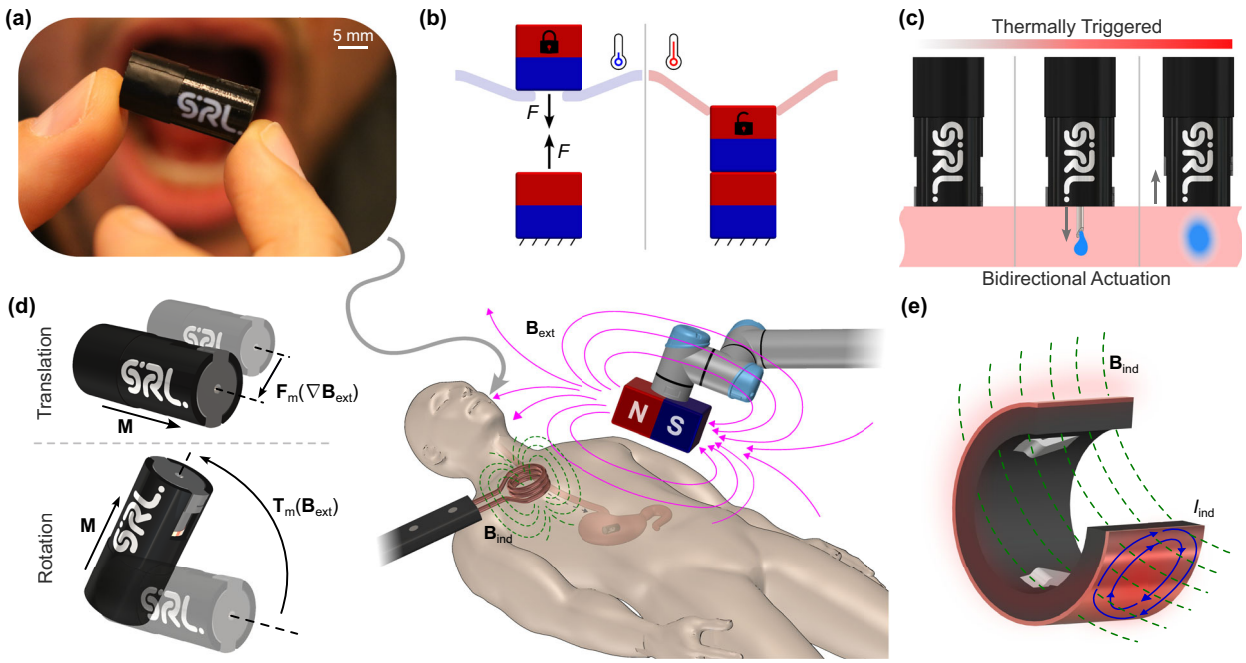

Fig. 1 | Inductively triggered capsule robot for needle-based drug delivery using thermally triggered magnetic springs (TTMS). a Image of the proposed millimeter-scale capsule robot. **c** Bidirectional needle actuation enabled by embedding multiple TTMSs. **b** Schematic of a thermally triggered magnetic spring (TTMS), consisting of a preloaded magnetic spring and a temperature-responsive locking structure. **d** Contactless magnetic steering of the capsule through interaction between the internal magnetic moment (**M**) and an external magnetic field (**B**), generating magnetic forces ($\mathbf{F}_m$) and torques ($\mathbf{T}_m$). **e** Contactless inductive heating of conductive components via eddy currents (I_{ind}) induced by an oscillating magnetic field ($\mathbf{B}_{ind}$), enabling thermal triggering of TTMS. Human models adapted under CC BY 4.0 from Simoslay (Sketchfab) and Johnson J (NIH 3D Print Exchange).

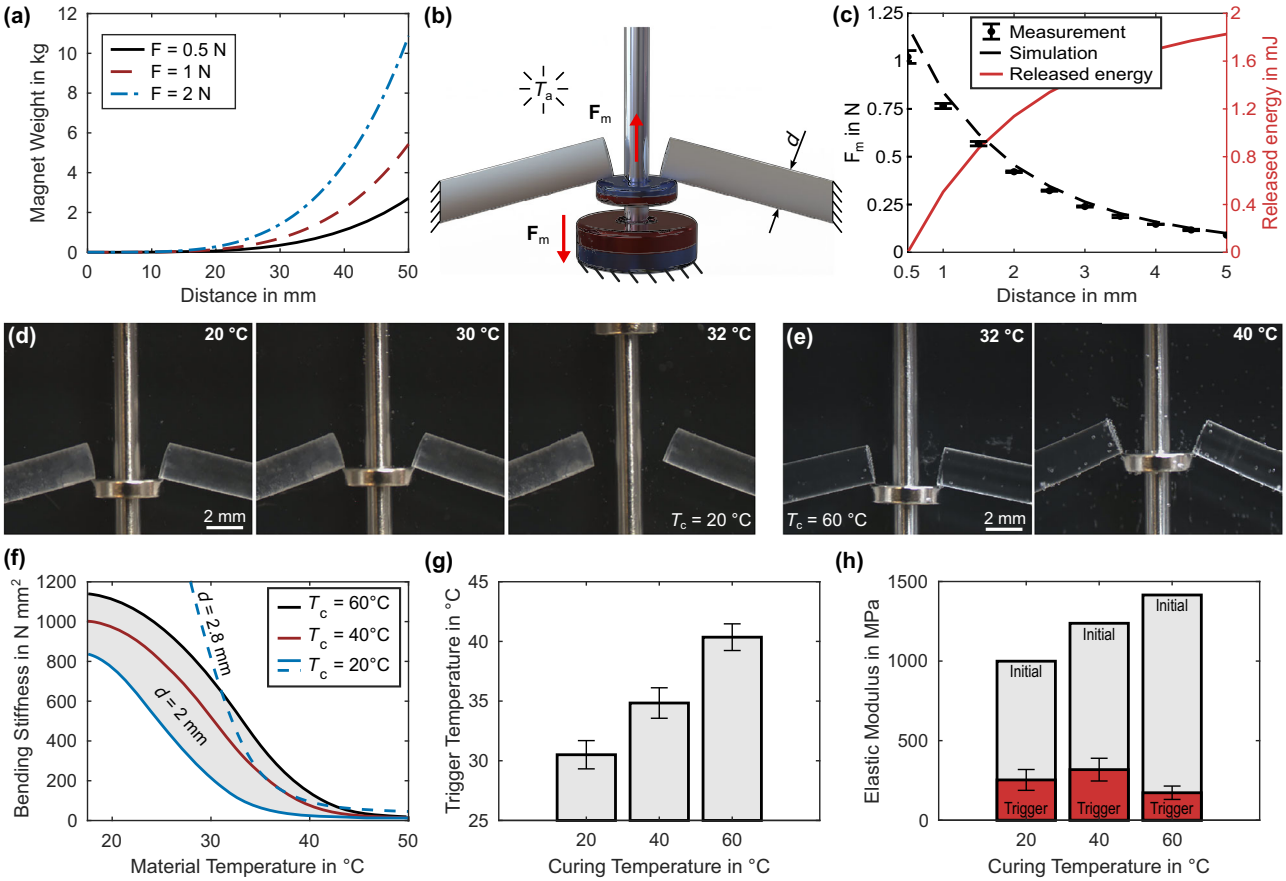

Fig. 2 | Local force generation using thermally triggered magnetic springs (TTMS). a Required mass of an external permanent magnet to generate a given force (F) on a milli-scale cylindrical permanent magnet as a function of distance. Please refer to Supplementary Note 2 for a detailed description. **b** Schematic of the simplified TTMS consisting of two beams with a diameter (d) of 2 mm made from NOA 63 and two permanent magnets repelled by magnetic force ($\mathbf{F}_m$). **c** Simulated and experimentally measured local actuation force ($\mathbf{F}_m$) and corresponding released potential energy of the simplified TTMS. **d**, **e** Representative programmable thermal triggering of simplified TTMS cured at 20 °C and 60 °C. Please refer to Supplementary Movie 1 for demonstration of the TTMS concept. **f** Temperature-dependent bending stiffness of NOA63 beams with different curing temperatures (T_c). **g** Trigger temperature of simplified TTMS cured at 20, 40, and 60 °C. **h** Elastic modulus of the locking beams at room temperature (grey) and at the trigger temperature (red).

magnetic stainless steel rod, allowing free axial motion while preventing pole alignment. As the ambient temperature increases, the softening of the NOA63 beams leads to increasing deformation under magnetic preload (Fig. 2d and Supplementary Movie 1) until the trigger temperature (T_t) is reached and the magnetic spring is released. By adjusting the curing temperature, T_t can be programmed to meet application-specific requirements or to enable multi-step actuation sequences (Fig. 2e).

We characterize the thermal trigger behavior and the programmability of TTMS with beams cured at three different temperatures ($T_c \in [20, 40, 60]$ °C). Beams cured at 60 °C exhibit a 40% higher bending stiffness at room temperature and a 300% higher stiffness at 30 °C compared to beams cured at 20 °C (Fig. 2f). Achieving a comparable stiffness increase at 30 °C using a beam cured at 20 °C would require an increase in beam diameter of approximately 40%. The curing-dependent stiffness directly influences the trigger temperature of the TTMS (Fig. 2g). Increasing T_c from 20 °C to 60 °C results in an increase in T_t of approximately 10 °C, while the elastic moduli at T_t remain similar (Fig. 2f). The direct relationship between curing temperature and trigger temperature enables the realization of geometrically identical TTMS with distinct, programmable activation thresholds. Moreover, the presented locking structures can be readily miniaturized, allowing multiple TTMS with identical or distinct trigger behavior to be integrated into millimeter-scale untethered robotic systems, with heat serving as the sole actuation trigger.

Thermal-magnetic responsive capsule

The proposed capsule robot integrates multiple thermally triggered magnetic springs (TTMS) to enable contactless, sequential needle-based drug injection into soft tissue (Fig. 1c). Two miniaturized TTMSs are used to sequentially control needle ejection and retraction (Fig. 3a). Structurally, the system consists of an inner capsule and an outer shell (Fig. 3b). The inner capsule contains the injection needle, three permanent magnets, and the TTMS responsible for ejecting the needle. The outer shell houses a single permanent magnet and the TTMS responsible for retracting the needle. In addition to local actuation, the magnets of the TTMS enable contactless magnetic steering under a quasi-static external magnetic field (Fig. 1d). The TTMS are triggered by inductive heating of 50 µm-thick copper elements embedded in the capsule using an oscillating magnetic field at 16 kHz (Fig. 1e).

In the envisioned clinical workflow, the capsule is first steered magnetically toward the target region using a quasi-static field generated by a magnetic actuation system compatible with human-sized workspaces[48,49]. Only once the target location has been reached is an alternating magnetic field generated to trigger the capsule inductively, preventing premature needle ejection. Since magnetic steering and inductive heating operate in fundamentally different frequency regimes, the two subsystems are physically decoupled and can be operated without mutual interference, as demonstrated in previous studies[50,51].

The actuation sequence of needle ejection and retraction is controlled by embedding multiple TTMS with distinct trigger temperatures. The

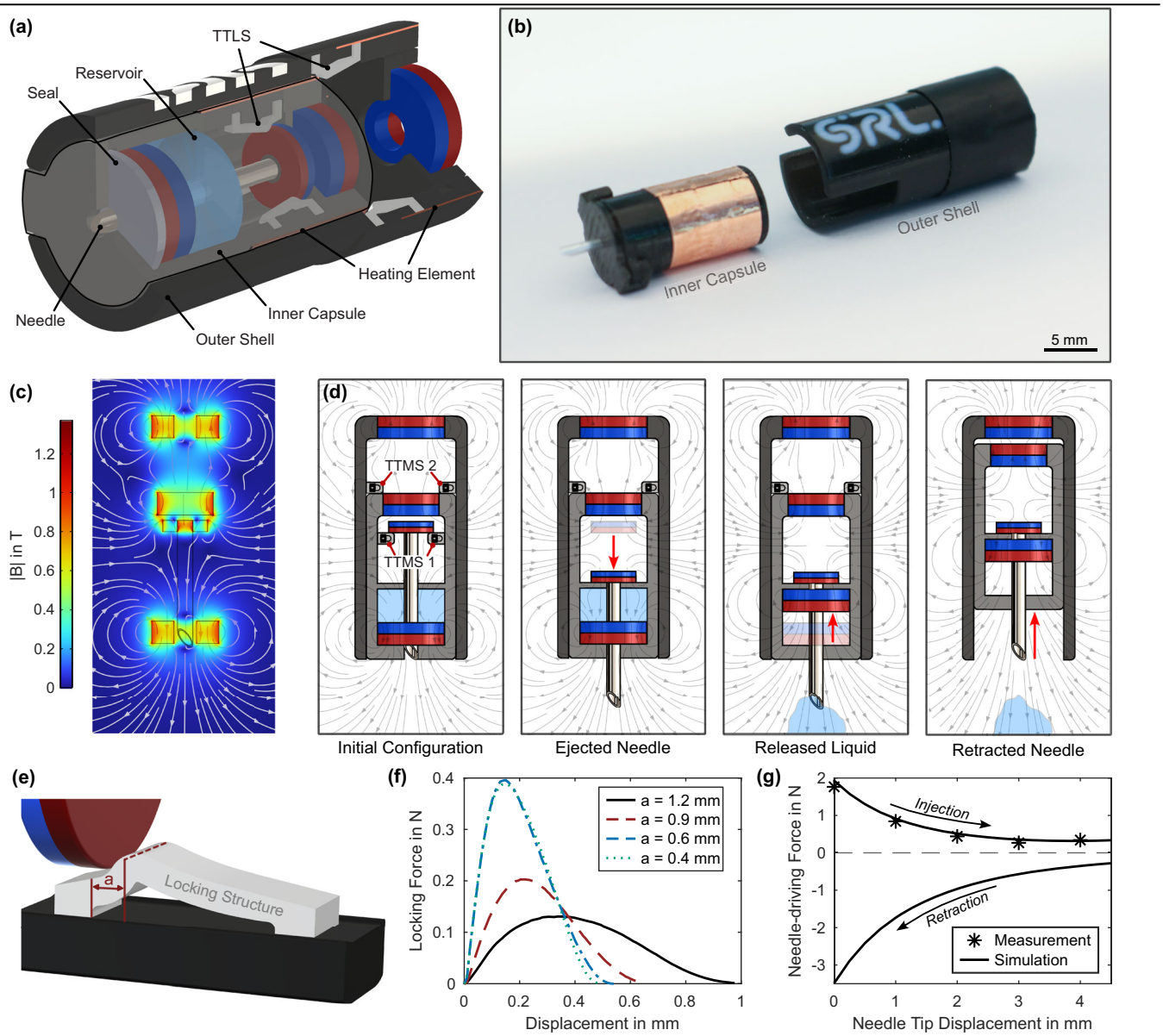

Fig. 3 | Capsule robot design and sequential actuation for needle-based drug delivery. a Design overview of the proposed capsule robot. **b** Display of the two principal components of the capsule robot: the inner capsule and the outer shell. **c** Simulated magnetic flux density in the initial capsule configuration. **d** Schematic of the thermally triggered actuation sequence enabled by two thermally triggered magnetic springs. **e** Design of a miniaturized thermally triggered locking structure (TTLS) with an edge-to-peak distance (*a*) of 0.6 mm. **f** Finite element-based parametric analysis of the influence of *a* on locking force and force gradient. **g** Simulated and experimentally measured forces during needle ejection and retraction.

trigger temperature of each TTMS depends on both its magnetic configuration and the curing conditions of the embedded thermally triggered locking structures (TTLS) (Fig. 3c). Upon heating, the first TTMS is activated, generating a pushing force that drives the needle into the tissue (Fig. 3d). Continued heating subsequently activates the second TTMS, which produces a pulling force that retracts the needle. Both needle ejection and retraction are triggered by a single global thermal stimulus, without the need to individually address the actuators.

To accommodate multiple TTMS within the limited volume of the milli-scale capsule, the design incorporates miniaturized TTLS, replacing the simplified beam-based locking structures used in the previous section (Fig. 3e and Supplementary Fig. 5). Each TTMS consists of three TTLS arranged circumferentially around the longitudinal axis of the capsule. The TTLS is designed to support bidirectional operation, which is necessary to lock, trigger, and reload the capsule without requiring disassembly. Bidirectional operation is enabled through locking elements with bridge-like geometry. A finite element-based parametric analysis is conducted to determine the optimal edge-to-peak distance that maximizes the locking force and force gradient, thereby enabling a large free stroke while avoiding unnecessary small geometric features that do not provide additional performance gains (Supplementary Note 2). Based on the parametric analysis, an edge-to-peak distance of 0.6 mm is selected (Fig. 3f). In this configuration, the peak locking force is reached after approximately 0.2 mm, resulting in an available free stroke of 4.3 mm for the TTMS. By minimizing the displacement needed to reach the locking force peak, the force output and usable potential energy for actuation are maximized.

The needle ejection is driven by two oppositely magnetized permanent magnets, closely positioned together in the preloaded state. The magnetic interaction between all embedded magnets is analyzed numerically (Supplementary Note 3). When the first TTMS is triggered, the repelling magnets initially generate a maximum driving force that decreases from approximately 2 N to 0.5 N as the needle is deployed (Fig. 3g). Needle insertion follows a four-stage mechanical process consisting of loading deformation, rupture, cutting, and unloading. The insertion force peaks during rupture

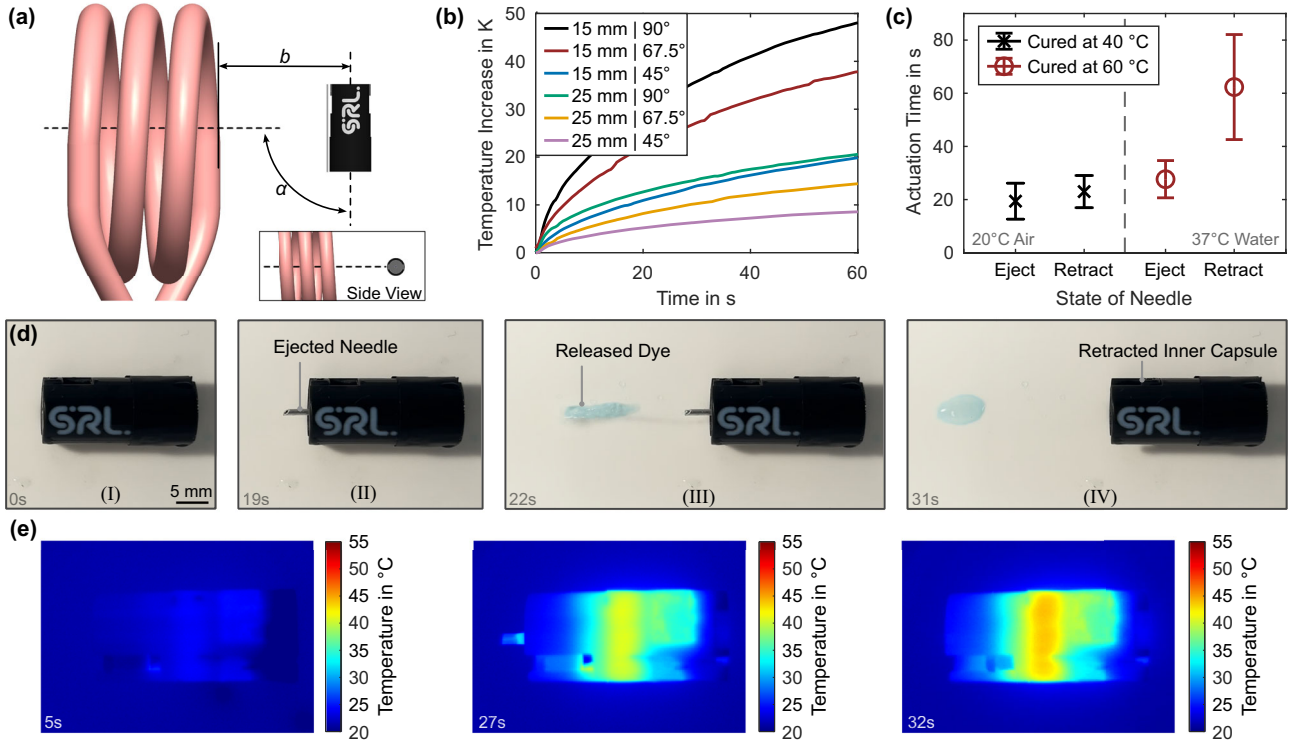

Fig. 4 | Validation of inductively triggered sequential actuation. a Schematic of experimental setup used to characterize inductive heating depending on capsule distance (b) and orientation (α). **b** Measured capsule surface temperature over time for different b and α. **c** Trigger times required to complete the full actuation sequence for two capsules with different programmed trigger temperatures in air and warm water. **d** Representative actuation sequence: (I) initial state, (II) needle ejection, (III) dye release, and (IV) needle retraction. **e** Thermal images at representative actuation states. Please refer to Supplementary Movie 2 for demonstration of the full actuation sequence.

and is proportional to tissue toughness, inversely proportional to needle radius, and influenced by friction and insertion velocity, with the primary contributing forces being tissue deformation, tearing, and frictional resistance. Because tissue puncture requires the highest force at the initial penetration of the outer surface[52], and the driving force varies with needle position, using repelling rather than attracting magnets ensures that the peak force is applied at the beginning of the motion and prevents the needle from stalling before sufficient force is reached to penetrate the tissue. An additional magnet, magnetized in the same direction as the needle magnet, is introduced to sustain a minimum driving force and enable drug injection. This magnet compresses the internal drug reservoir following needle deployment and is held in place through friction. As the needle is ejected, the acting magnetic force between the needle magnet and the compression magnet increases, eventually overcoming the acting friction, leading to compression of the reservoir. Reservoir compression, and thus fluid release, occurs only after the needle is ejected, ensuring that injection is initiated within the tissue. A sealing pad attached to the secondary magnet prevents premature leakage and increases internal friction for controlled release.

After needle injection and further temperature increase, the second TTMS is activated to retract the needle. In contrast to the ejection mechanism, which relies on repelling magnets to generate a high initial force, the TTMS for retracting the needle employs two coaxially magnetized magnets initially separated by a distance of 5 mm. This configuration produces a lower initial force of approximately 0.4 N, which progressively increases up to 3.5 N during actuation, causing the needle to retract and the inner capsule to slide into the outer shell. This controlled retraction prevents unwanted interaction between the needle and the surrounding tissue after the drug is injected.

Inductively triggered sequential actuation

Contactless triggering of the capsule robot is essential for potential medical applications. In our system, contactless triggering is achieved by inductive heating of embedded copper elements. When exposed to a high-frequency oscillating magnetic field, eddy currents are induced in these elements, resulting in a controlled temperature increase because of Joule heating. By combining inductive heating with multiple thermally triggered magnetic springs (TTMS), the capsule achieves bidirectional needle motion without the application of external magnetic forces or torques.

First, we characterize the inductive heating performance of the capsule for different orientations and distances relative to an induction coil (Fig. 4a). At a coil-capsule distance (b) of 25 mm and with the capsule axis perpendicular to the central axis of the coil (α = 90°), a temperature increase of approximately 20 °C is observed after 60 s of heating (Fig. 4b). This increase in temperature corresponds to a reduction in material stiffness of approximately 75 – 85% in the employed TTMSs. The heating performance strongly depends on the relative orientation between the capsule and the induction coil. Maximum heating is achieved when the capsule axis is perpendicular to the coil, while at an orientation angle of 45°, the heating capability decreases by approximately 50%. Nevertheless, even at a distance of 25 mm and a misalignment of 45°, a temperature increase of approximately 10 °C is achieved, corresponding to a reduction in stiffness of up to 50%. These results demonstrate that inductive heating can significantly reduce the stiffness of TTMS and serve as a contactless trigger for the capsule actuation mechanism.

Secondly, we validate whether the bidirectional actuation sequence required for needle deployment, drug release, and needle retraction can be thermally triggered using inductive heating. For this experiment, the embedded magnetic springs are preloaded, and the reservoir is filled with a dyed liquid to visualize needle-based drug injection. At a surface temperature of 40 °C, the first TTMS is triggered, which results in needle ejection followed by the compression of the drug reservoir and visible dye ejection through the needle (Fig. 4d, e and Supplementary Movie 2). Continued heating subsequently activates the second TTMS at 45 °C, resulting in controlled needle retraction by pulling the inner capsule into the outer shell.

Fig. 5 | Demonstration of targeted needle-based drug delivery and navigation. **a** Locomotion strategy of the capsule robot can be adapted to different types of obstacles encountered during navigation. Please refer to Supplementary Movie 3 for demonstration of the locomotion capabilities. **b** Contactless inductively triggered puncture and dye injection into a soft tissue mimic. Please refer to Supplementary Movie 4 for a complete demonstration. **c** Contactless inductively triggered puncture into ex vivo porcine stomach tissue. Please refer to Supplementary Movie 5 for demonstration of the ex vivo capabilities of the capsule. **d** Tissue surface before and after puncture, showing the penetration mark created by the needle. **e** Magnetic navigation of the capsule robot along a spiral trajectory on the inner surface of a porcine stomach.

This experiment validates the functionality of the proposed TTMS-based sequential actuation concept and demonstrates controllable bidirectional needle motion in a capsule robot.

Finally, we evaluate the programmability of the capsule's thermal response and thus the adaptability to different environmental conditions. We compare two capsules incorporating TTMS cured at different temperatures: one cured at 40 °C for operation in air at room temperature, and one cured at 60 °C for operation in aqueous media at normal gastrointestinal temperature (37 °C) (Fig. 4c)[53]. At room temperature, the 40 °C-cured capsule shows needle ejection after an average of 19 ± 6.7 s of inductive heating and needle retraction after 23 ± 6.1 s. In contrast, the 60 °C-cured capsule cannot be triggered under the same conditions, even with prolonged heating, due to insufficient softening of the embedded TTMS. When operated in water at 37 °C, the 60 °C-cured capsule becomes fully functional,

showing needle ejection after 30 ± 7.0 s and retraction after 60 ± 19.8 s of inductive heating (Supplementary Fig. 6). Conversely, the 40 °C-cured capsule is triggered prematurely when placed into the warm water. These results show that the thermal response of the capsule can be programmed to different environments without requiring changes to the overall design or material composition, highlighting the adaptability of our proposed actuation approach.

Towards targeted soft tissue drug injection

The capsule robot must be able to penetrate tissue to enable localized injection for targeted drug delivery. Furthermore, it must be capable of navigating through a three-dimensional environment to reach a target location. We are therefore investigating the capabilities of the capsule in terms of tissue penetration, fluid injection, magnetic steering, and obstacle traversal.

The TTMSs integrated into the capsule incorporate multiple permanent magnets that serve both for localized actuation and for magnetic navigation. By applying an external magnetic field, the capsule can be translated, oriented, and rolled. Translational motion is achieved through magnetic field gradients that generate a pulling force on the capsule, while orientation and rolling arise from magnetic torque induced by the interaction between the capsule's magnetic moment and the applied field. The combination of pulling and rolling enables versatile locomotion strategies, allowing the capsule to adapt its motion to obstacles of varying geometry and height.

We first validate the locomotion capability of the capsule in a controlled maze environment containing three distinct obstacles (Fig. 5a and Supplementary Movie 3). For this, the capsule is steered using a handheld permanent magnet. The first obstacle requires lateral maneuvering around the obstruction, while the second and third obstacles require crossing elevated elements. Depending on the height of the obstacle, the capsule can either slide over it or, if sliding is not possible, roll over it. These experiments demonstrate adaptable locomotion strategies enabled by combined magnetic pulling and rolling.

After reaching a target site, the capsule must generate sufficient force to penetrate tissue and inject the loaded liquid into the tissue rather than releasing it onto the surface. We evaluate puncture and injection performance using a transparent soft tissue mimic fabricated from 1.5 wt% agar (Fig. 5b and Supplementary Movie 4). The capsule is placed on the surface of the soft tissue mimic and inductively heated. After heating the capsule for 34s, the first TTMS is triggered, resulting in the needle puncturing through the tissue mimic and the loaded dye being ejected. Additional heating for 6 seconds triggers the second TTMS, which retracts the needle and returns the capsule to a safe state so that it can continue to be moved through a surrounding environment. This experiment confirms that the capsule can penetrate tissue-mimicking material and perform liquid injection followed by controlled retraction.

Finally, we evaluate the capsule performance in real biological tissue using an ex vivo porcine stomach. First, we assess the locomotion capability within the three-dimensional geometry of the stomach. We use a handheld magnet to steer the capsule along a spiral trajectory toward the center of the stomach (Fig. 5e and Supplementary Movie 5). By combining both magnetic pulling and rolling, the capsule successfully navigates across the natural rugae. This demonstrates the ability of the capsule to navigate complex, compliant, and uneven tissue surfaces. Secondly, we assess the puncturing capability with biological tissue. A section of porcine stomach is positioned beneath the capsule, and the capsule is triggered inductively. After 32s of inductive heating, the needle is ejected, visibly deforming and puncturing the tissue (Fig. 5c and Supplementary Movie 5). Once the capsule is removed, a clear puncture remains visible on the tissue surface (Fig. 5d). Together, these experiments demonstrate that the capsule can be magnetically navigated within a gastrointestinal environment and can penetrate biological tissue, providing a critical step toward targeted drug delivery through physiological barriers.

Discussion

We present a programmable millimeter-scale capsule robot capable of controlled needle-based drug delivery. By integrating multiple TTMS into a single capsule robot, the system performs a programmable multi-step actuation sequence that ejects a needle, releases a liquid payload, and subsequently retracts the needle. Each TTMS combines a preloaded magnetic spring with a temperature-responsive locking structure, allowing thermally triggered multi-newton force generation. Fully contactless triggering of the capsule robot is achieved through inductive heating.

The TTMS-based design offers several key advantages for capsule robots used in applications requiring actuation forces in the multi-newton range. Unlike external actuation approaches, in which the achievable force decreases with increasing source-to-capsule distance, the locally generated actuation force remains independent of the external system, making the approach scalable to clinical-scale workspaces. The thermal response of each TTMS can furthermore be programmed during fabrication by adjusting the curing temperature of the locking structure, allowing the trigger temperature to be tuned without affecting the force output and enabling the design of sequential actuation sequences. In addition, the embedded permanent magnets can be used for magnetic steering, allowing navigation without integrating additional magnetic components. The decoupling between navigation and actuation furthermore enables the capsule to maintain full magnetic maneuverability while locally generating sufficient forces for puncturing tissue, demonstrating that TTMS is a viable actuation strategy for untethered capsule robots requiring multi-newton force generation.

Experimental results demonstrate that our capsule robot can penetrate soft tissue mimics and puncture ex vivo porcine stomach tissue, showing the ability to overcome physiological barriers relevant for targeted drug delivery. Contactless activation through inductive heating enables controlled triggering of the actuation sequence, and we further demonstrate liquid payload ejection through the deployed needle. By adjusting the curing conditions of the embedded locking structures, the thermal response of the capsule robot is adapted to environments with different temperatures, including dry and aqueous conditions, demonstrating suitability for operation in physiological environments. In addition, we demonstrate locomotion strategies based on magnetic pulling and rolling, which enable the capsule to move in complex three-dimensional environments and navigate over compliant, uneven biological surfaces, as shown in ex vivo porcine stomach experiments. Together, these results demonstrate that the capsule robot combines controlled tissue interaction, programmable actuation, and magnetic navigation within a compact millimeter-scale system.

Compared with previously reported capsules for needle-based drug delivery, which rely on passive environmental triggers or externally applied magnetic forces, the presented capsule enables controlled needle ejection and retraction through inductive triggering while preserving magnetic navigation capability. In our approach, inductive heating is needed only to trigger the capsule, while the actuation force and thus the ability to penetrate tissue and deliver a payload remain independent of the external system. Consequently, the combination of local force generation, magnetic steering, and inductive triggering provides a level of operational control and functional independence that extends beyond previously reported capsule robots for needle-based drug delivery.

Expanding on the presented ex vivo demonstrations, further in vivo studies are required to evaluate the performance of the capsule robot under realistic physiological conditions. In particular, inductive heating for contactless triggering introduces constraints in terms of both heating performance and thermal safety. The heating efficiency depends on the pose of the capsule relative to the external induction coil, such that unfavorable alignment can reduce the achievable capsule temperature. In addition, the thermal load applied to surrounding tissue during triggering must be carefully managed to avoid thermal damage to biological tissue. In the envisioned in vivo application, knowledge of the capsule pose is inherently required for magnetic navigation. This information can therefore be directly used to adapt the heating process. By adjusting the position

and orientation of the induction coil as well as the heating duration, reduced heating efficiency at unfavorable capsule poses can be compensated. Ultrasound imaging provides a practical solution for obtaining pose feedback of the capsule and has been shown to be compatible with both magnetic steering and inductive heating of untethered robots in vivo[50,51]. Several design modifications could further improve heating performance, thermal safety, and readiness for in vivo deployment. For example, increasing the volume of conductive material within the capsule could enhance heating efficiency and extend the operating distance between induction coil and capsule, while relocating the heating elements further toward the inside of the capsule would improve thermal isolation and reduce peak surface temperatures. Further miniaturization of TTMS could reduce the overall capsule size, broadening the range of accessible anatomical regions. In addition, the integration of embedded sensing could support feedback-driven control of capsule pose and actuation state, reducing reliance on external visualization and improving the safety and reliability of drug injection. Together, these developments would make the capsule robot suitable for in vivo deployment.

Beyond the presented application in a capsule for needle-based drug delivery, TTMS represents a generalizable actuation building block for untethered robotic systems and can be applied to other medical interventions, including biopsy and drainage. By decoupling strong local actuation from external magnetic force generation, TTMS addresses a key limitation in the design of medical capsule robots. More broadly, the ability to design compact actuators with programmable force magnitude, direction, and trigger temperature could enable multifunctional milli-scale robots capable of complex, sequential behaviors triggered by a single global stimulus.

Methods

Fabrication of thermally responsive locking structure

The thermally triggered locking structures are made from a bio-compatible, UV-curable polyurethane-based shape memory polymer (NOA63, Norland Products Inc, United States). Both the locking beams and the miniaturized locking structures used in the capsule are molded. Commercially available silicone tubing is used as a mold for manufacturing the beams. The miniaturized locking structures, however, are molded using custom-made molds made from 2 mm-thick polydimethylsiloxane (PDMS) (Sylgard 184, Dow, United States) sheets, which themselves undergo a molding procedure. These sheets are made by mixing PDMS at a 10:1 volume ratio of base-curing agent. After curing, the shape of the locking structures is laser-engraved (Speedy 300, Trotec Laser, Austria) into the prepared PDMS sheets. Three engraving steps are performed to achieve the desired engraving depth of 1 mm. After engraving, the molds are flushed with water to remove residue. Subsequently, NOA63 is poured into the engraved cavity. Afterwards, the filled mold is vacuumed for 5 min at 100 mbar to remove any air bubbles. Finally, the filled mold is pre-heated for 5 min at either 20, 40 or 60 °C, followed by a 30-min UV-A light exposure at either 20, 40 or 60 °C. Afterwards, the SMP is solidified and fully cured. Upon cooling, the locking structures can be manually extracted from the PDMS mold.

Fabrication of thermal-magnetic responsive capsule

The proposed capsule robot consists of an inner capsule and an outer shell. The capsule has a cylindrical geometry with an outer diameter of 10 mm and a length of 21 mm. Both the inner capsule and outer shell are made from multiple 3D-printed components bonded together. All 3D-printed components are printed with a PolyJet printer (J750, Stratasys, USA). The miniaturized locking elements and all permanent magnets are manually embedded and bonded to the 3D-printed components using adhesive (LOCTITE 401, Henkel Adhesive Technologies, Germany). The needle is custom-made from a $\varnothing$ 1 mm aluminum tube and has a total length of 12 mm, of which 4.5 mm is ejected upon actuation. The needle tip is sharpened, and an opening for drug release is drilled. The magnet used to compress the reservoir is glued to a 3D-printed sealing pad, which also serves as a guide for the needle. Single-sided adhesive copper tape with a thickness of 0.05 mm (VIVIIHOO, China) wrapped around the inner capsule and outer shell. The copper tape wrapped around the outer shell is covered with isolating tape (165BK4A, 3M, USA). The TTMS used to eject the needle is loaded by placing the inner capsule in warm water and pushing the needle into the capsule. Once the needle is pushed in, the capsule is placed in cold water to lock the needle in place.

Demonstration of simplified TTMS

We validate the TTMS concept and evaluate the programmability using three simplified TTMS programmed with different curing temperatures. Each TTMS comprises a symmetric pair of identical locking beams fabricated from NOA63 and two axially repelling ring magnets (N45: 6 × 2 × 2 mm, N48: 4 × 1.4 × 1 mm). The magnets are aligned and guided by a stainless-steel rod and embedded, together with the locking beams, in a rigid outer frame. The locking beams (length: 15 mm, diameter: 2 mm) are fabricated following the procedure described above and cured at 20, 40, or 60 °C. The programmability is evaluated by comparing the deformation of the locking beams under identical magnetic load. For testing, each preloaded TTMS is submerged in a temperature-controlled water bath, with the water temperature continuously monitored using a digital temperature sensor (DS18B20, Maxim Integrated Products, USA). The temperature-dependent deformation of the beams is recorded using an external camera. In all experiments, the initial water temperature is approximately 16 °C and is increased quasi-statically until TTMS release occurs. Each TTMS is tested five times to assess repeatability.

Characterization of inductive heating performance

We characterize the inductive heating capability of our capsule by measuring the surface temperature when exposed to a high-frequency oscillating magnetic field. The oscillating magnetic field is generated with a water-cooled induction coil. The induction coil generates a field with a frequency of 16 kHz and a power of 400 W. The surface temperature of the capsule is measured and recorded using an infrared camera (Ti400, Fluke Corporation, USA). The recorded images are post-processed using MATLAB 2023b (The MathWorks, USA).

Measurement of needle-driving force

The needle driving force is measured using a custom-built setup. An adapted capsule with a 15 mm long, blunt needle is fixed and positioned using a laser-cut experimental setup. The tip of the needle is connected through an adapter to a force sensor. The needle position is controlled by adjusting the capsule position with an linear stage. The force acting on the needle is measured using a 3-axis force sensor (K3D40a, ME-Messsysteme GmbH, Germany) and a signal amplifier (GSV-4USB, ME-Messsysteme GmbH, Germany).

Validation of actuation sequence

The sequential actuation concept is validated by inductively heating the fully assembled capsule robot and observing the sequential ejection and retraction of the needle. The capsule is placed on a flat surface under ambient conditions, with its longitudinal axis oriented perpendicular to the central axis of the induction coil and an actuation distance of 20 mm between the coil and the central axis of the capsule. The capsule is loaded with a blue dye to visualize fluid ejection and continuously heated at a frequency of 16 kHz and a power of 400 W until completion of a full actuation cycle, defined as needle ejection followed by subsequent needle retraction. The surface temperature of the capsule is monitored throughout the experiment using an infrared camera (Ti400, Fluke Corporation, USA), and the recorded thermal images are post-processed using MATLAB 2023b (The MathWorks, USA).

Characterization of capsule trigger time

The trigger time of the capsule robot is quantified for two differently programmed configurations (T_C = 40 °C and T_C = 60 °C). The capsule equipped with TTMS cured at 40 °C is actuated in air at room temperature, whereas the capsule equipped with TTMS cured at 60 °C is actuated in a

temperature-controlled water bath maintained at 37.5 °C to approximate physiological conditions. In all experiments, the longitudinal axis of the capsule is oriented perpendicular to the rotational axis of the induction coil, and the actuation distance between the coil and the capsule is fixed at 15 mm. The capsule is continuously heated inductively until completion of a full actuation cycle, defined as both needle ejection and subsequent retraction. The triggering time is measured from the onset of inductive heating to the completion of this cycle. Each capsule configuration is tested five times to assess repeatability.

Magnetic navigation

Magnetic steering of the capsule is achieved by exploiting the force and torque acting on a magnetic dipole in an external magnetic field. When a magnetic moment $\mathbf{m}$ is exposed to an external magnetic field ($\mathbf{B}_{ext}$), a magnetic force ($\mathbf{F}_m = \mathbf{m} \cdot \nabla \mathbf{B}_{ext}$) results from spatial field gradients, enabling translational pulling. In addition, a magnetic torque ($\mathbf{T}_m = \mathbf{m} \times \mathbf{B}_{ext}$) acts to align the magnetic moment with the applied field, which can be used for orienting and rolling the capsule. By combining magnetic pulling and rolling, the capsule can maneuver around and overcome obstacles of varying geometry and height.

In the proposed capsule robot, the permanent magnets integrated within the TTMS serve both as local actuators and as magnetic dipoles for external steering. The external magnetic field is generated using an axially magnetized cylindrical permanent magnet (diameter: 30 mm, length: 150 mm, N52). In all experiments, the magnet is positioned below the test setup, and its position and orientation relative to the capsule are adjusted manually.

Demonstration of soft tissue puncturing and liquid release

The needle-based drug delivery capability of the capsule robot is evaluated in two representative scenarios. In both scenarios, the capsule is placed directly on the material to be punctured and inductively heated following the procedure described before. To stabilize the capsule during needle ejection, a lateral magnetic force of approximately 65 mN is applied by an additional external permanent magnet positioned behind the vertical wall of the experimental setup. This keeps the capsule upright and in stable contact with the tissue surface below. In the first experiment, the capsule is loaded with 100μL of water mixed with blue dye and positioned on top of an agar-based tissue mimic. Upon thermal triggering, the capsule punctures the agar sheet and injects the dye into an underlying polyvinyl alcohol (PVA) sponge, serving as a compliant reservoir. Agar sheets are prepared by dissolving 1.5 wt% agar powder in water, heating the mixture to boiling, and casting it into molds. After solidification, the sheets are stored submerged in water at 6 °C until use. In the second experiment, the puncturing of biological tissue is assessed using ex vivo porcine stomach samples. The capsule is positioned on the surface of the tissue and inductively heated until needle ejection into the tissue is observed. After actuation, the capsule is removed, and the tissue surface is optically inspected to assess the puncture.

Data availability

All data supporting the findings of this study are available in this manuscript and its Supplementary Information.

Received: 16 March 2026; Accepted: 26 May 2026;
Published online: 03 June 2026

References

1. Kavic, S. M. & Basson, M. D. Complications of endoscopy. *Am. J. Surg.* **181**, 319–332 (2001).
2. Borner, M. et al. Patient preference and pharmacokinetics of oral modulated UFT versus intravenous fluorouracil and leucovorin. *Eur. J. Cancer* **38**, 349–358 (2002).
3. Mignani, S., El Kazzouli, S., Bousmina, M. & Majoral, J.-P. Expand classical drug administration ways by emerging routes using dendrimer drug delivery systems: a concise overview. *Adv. Drug Deliv. Rev.* **65**, 1316–1330 (2013).
4. Wiarda, B. M. et al. Patient burden and patient preference: comparing magnetic resonance enteroclysis, capsule endoscopy and balloon-assisted enteroscopy. *J. Gastroenterol. Hepatol.* **28**, 464–471 (2013).
5. Iddan, G., Meron, G., Glukhovsky, A. & Swain, P. Wireless capsule endoscopy. *Nature* **405**, 417–417 (2000).
6. Eliakim, R., Yassin, K., Shlomi, I., Suissa, A. & Eisen, G. M. A novel diagnostic tool for detecting oesophageal pathology: the PillCam oesophageal video capsule. *Aliment. Pharmacol. Ther.* **20**, 1083–1089 (2004).
7. Gopalakrishnan, S. et al. Smart capsule for monitoring inflammation profile throughout the gastrointestinal tract. *Biosens. Bioelectron. X* **14**, 100380 (2023).
8. Wang, Z. Ingestible electrochemical sensors: emerging tools for gastrointestinal disease detection and monitoring. *Int. J. Electrochem. Sci.* **20**, 100952 (2025).
9. Cao, Q. et al. Robotic wireless capsule endoscopy: recent advances and upcoming technologies. *Nat. Commun.* **15**, 4597 (2024).
10. Kadian, S. et al. Smart capsule for targeted detection of inflammation levels inside the GI tract. *IEEE Trans. Biomed. Eng.* **71**, 1565–1576 (2024).
11. Liao, Z. et al. Accuracy of magnetically controlled capsule endoscopy, compared with conventional gastroscopy, in detection of gastric diseases. *Clin. Gastroenterol. Hepatol.* **14**, 1266–1273.e1 (2016).
12. Shamsudhin, N. et al. Magnetically guided capsule endoscopy. *Med. Phys*. **44**, e91-e111 (2017).
13. Zhang, Y., Zhang, Y. & Huang, X. Development and application of magnetically controlled capsule endoscopy in detecting gastric lesions. *Gastroenterol. Res. Pract.* **2021**, 1–7 (2021).
14. Wang, X. et al. A systematic review on diagnosis and treatment of gastrointestinal diseases by magnetically controlled capsule endoscopy and artificial intelligence. *Ther. Adv. Gastroenterol.* **16**, 17562848231206991 (2023).
15. Zhang, F. et al. Gastrointestinal tract drug delivery using algae motors embedded in a degradable capsule. *Sci. Robot.* **7**, eabo4160 (2022).
16. Park, S., Hoang, M. C., Kim, J. & Park, S. Multiple sampling capsule robot for studying gut microbiome. *Adv. Intell. Syst*. **7**, 2300625 (2024).
17. Son, D., Gilbert, H. & Sitti, M. Magnetically actuated soft capsule endoscope for fine-needle biopsy. *Soft Robot.* **7**, 10–21 (2020).
18. Hao, B. et al. Focused ultrasound enables selective actuation and newton-level force output of untethered soft robots. *Nat. Commun.* **15**, 5197 (2024).
19. Shokrollahi, P. et al. Blindly controlled magnetically actuated capsule for noninvasive sampling of the gastrointestinal microbiome. *IEEE/ASME Trans. Mechatron.* **26**, 2616–2628 (2021).
20. Nam, J., Lai, Y. P., Gauthier, L., Jang, G. & Diller, E. Resonance-based design of wireless magnetic capsule for effective sampling of microbiome in gastrointestinal tract. *Sens. Actuators A: Phys.* **342**, 113654 (2022).
21. Rehan, M. et al. Smart capsules for sensing and sampling the gut: status, challenges and prospects. *Gut* **73**, 186–202 (2024).
22. Vargason, A. M., Anselmo, A. C. & Mitragotri, S. The evolution of commercial drug delivery technologies. *Nat. Biomed. Eng.* **5**, 951–967 (2021).
23. Lee, J., Lee, H., Kwon, S. -h & Park, S. Active delivery of multi-layer drug-loaded microneedle patches using magnetically driven capsule. *Med. Eng. Phys.* **85**, 87–96 (2020).
24. Erin, O., Boyvat, M., Lazovic, J., Tiryaki, M. E. & Sitti, M. Wireless MRI-powered reversible orientation-locking capsule robot. *Adv. Sci.* **8**, 2100463 (2021).
25. Ze, Q. et al. Spinning-enabled wireless amphibious origami millirobot. *Nat. Commun.* **13**, 3118 (2022).

26. Song, S. et al. Integrated design and decoupled control of anchoring and drug release for wireless capsule robots. *IEEE/ASME Trans. Mechatron.* **27**, 2897–2907 (2022).
27. Zheng, L., Guo, S. & Kawanishi, M. Magnetically controlled multifunctional capsule robot for dual-drug delivery. *IEEE Syst. J.* **16**, 6413–6424 (2022).
28. Sun, Y. et al. Magnetically driven capsules with multimodal response and multifunctionality for biomedical applications. *Nat. Commun.* **15**, 1839 (2024).
29. Chen, Z. et al. A magnetic multi-layer soft robot for on-demand targeted adhesion. *Nat. Commun.* **15**, 644 (2024).
30. Yang, Z., Xu, C., Lee, J. X. & Lum, G. Z. Magnetic miniature soft robot with reprogrammable drug-dispensing functionalities: toward advanced targeted combination therapy. *Adv. Mater.* **36**, 2408750 (2024).
31. Zheng, Z. et al. Ultrasoft hydrogel immune millirobot with multimodal locomotion. *Sci. Adv.* **11**, eadw9133 (2025).
32. Boegh, M. & Nielsen, H. M. Mucus as a barrier to drug delivery - understanding and mimicking the barrier properties. *Basic Clin. Pharmacol. Toxicol.* **116**, 179–186 (2015).
33. Mohammed, Y. et al. Advances and future perspectives in epithelial drug delivery. *Adv. Drug Deliv. Rev.* **186**, 114293 (2022).
34. Kaffash, E., Shahbazi, M.-A., Hatami, H. & Nokhodchi, A. An insight into gastrointestinal macromolecule delivery using physical oral devices. *Drug Discov. Today* **27**, 2309–2321 (2022).
35. Van Gerwen, D. J., Dankelman, J. & Van Den Dobbelsteen, J. J. Needle-tissue interaction forces - a survey of experimental data. *Med. Eng. Phys.* **34**, 665–680 (2012).
36. Abramson, A. et al. A luminal unfolding microneedle injector for oral delivery of macromolecules. *Nat. Med.* **25**, 1512–1518 (2019).
37. Chen, W. et al. Dynamic omnidirectional adhesive microneedle system for oral macromolecular drug delivery. *Sci. Adv.* **8**, eabk1792 (2022).
38. Arrick, G. et al. Cephalopod-inspired jetting devices for gastrointestinal drug delivery. *Nature* **636**, 481–487 (2024).
39. Levy, J. A., Straker, M. A., Stine, J. M., Beardslee, L. A. & Ghodssi, R. Magnetically triggered ingestible capsule for localized microneedle drug delivery. *Device* **2**, 100438 (2024).
40. Zhou, H. & Alici, G. A magnetically actuated novel robotic capsule for site-specific drug delivery inside the gastrointestinal tract. *IEEE Trans. Syst. Man Cybern. Syst.* **52**, 4010–4020 (2022).
41. Erin, O. et al. Overcoming the force limitations of magnetic robotic surgery: magnetic pulse actuated collisions for tissue-penetrating-needle for tetherless interventions. *Adv. Intell. Syst.* **4**, 2200072 (2022).
42. Xiang, Y. et al. MINRob: a large force-outputting miniature robot based on a triple-magnet system. *IEEE Trans. Robot.* **40**, 3127–3145 (2024).
43. Huo, Y., Yang, L., Xu, T. & Sun, D. Design, control, and clinical applications of magnetic actuation systems: challenges and opportunities. *Adv. Intell. Syst.* **7**, 2400403 (2025).
44. Okamura, A., Simone, C. & O'Leary, M. Force modeling for needle insertion into soft tissue. *IEEE Trans. Biomed. Eng.* **51**, 1707–1716 (2004).
45. Davis, K. A., Burke, K. A., Mather, P. T. & Henderson, J. H. Dynamic cell behavior on shape memory polymer substrates. *Biomaterials* **32**, 2285–2293 (2011).
46. DiOrio, A. M., Luo, X., Lee, K. M. & Mather, P. T. A functionally graded shape memory polymer. *Soft Matter* **7**, 68–74 (2011).
47. Masjosthusmann, L., Richter, M., Makushko, P., Makarov, D. & Misra, S. Miniaturized variable stiffness gripper locally actuated by magnetic fields. *Adv. Intell. Syst.* **6**, 2400037 (2024).
48. Gervasoni, S. et al. A human-scale clinically ready electromagnetic navigation system for magnetically responsive biomaterials and medical devices. *Adv. Mater.* **36**, 2310701 (2024).
49. Martin, J. W. et al. Enabling the future of colonoscopy with intelligent and autonomous magnetic manipulation. *Nat. Mach. Intell.* **2**, 595–606 (2020).
50. Soon, R. H. et al. Pangolin-inspired untethered magnetic robot for on-demand biomedical heating applications. *Nat. Commun.* **14**, 3320 (2023).
51. Liu, X. et al. Miniature magneto-ultrasonic machines for wireless robotic sensing and manipulation. *Sci. Robot.* **10**, eadu4851 (2025).
52. Mahvash, M. & Dupont, P. Mechanics of dynamic needle insertion into a biological material. *IEEE Trans. Biomed. Eng.* **57**, 934–943 (2010).
53. Martins Januário, W., Prata, E. R. B. D. A., Natali, A. J. & Prímola-Gomes, T. N. Normal gastrointestinal temperature values measured through ingestible capsules technology: a systematic review. *J. Med. Eng. Technol.* **47**, 389–395 (2023).

Acknowledgements

This work is financially supported via the European Union's Horizon Europe Research and Innovation Programme, grant agreement #101070066 (project RÊGO).

Author contributions

L.M. conceived the idea, developed the design, conducted the simulation, carried out the experiments, and composed the manuscript. S.M. supervised the project and revised the manuscript.

Competing interests

The authors declare no competing interests.

Additional information

Supplementary information The online version contains supplementary material available at https://doi.org/10.1038/s44182-026-00097-w.

Correspondence and requests for materials should be addressed to Sarthak Misra.